

NASA TECHNICAL NOTE



NASA TN D-8528 c.1

NASA TN D-8528

LOAN COPY: RETN
AFWL TECHNICAL
KIRTLAND AFB,



ELASTOHYDRODYNAMIC LUBRICATION
OF ELLIPTICAL CONTACTS FOR
MATERIALS OF LOW ELASTIC MODULUS

I - Fully Flooded Conjunction

Bernard J. Hamrock and Duncan Dowson

Lewis Research Center

Cleveland, Ohio 44135

NATIONAL AERONAUTICS AND SPACE ADMINISTRATION • WASHINGTON





0134228

| | | |
|---|--|---|
| 1. Report No. NASA TN D-8528 | 2. Government Accession No. | 3. Recipient's Catalog No. |
| 4. Title and Subtitle ELASTOHYDRODYNAMIC LUBRICATION OF ELLIPTICAL CONTACTS FOR MATERIALS OF LOW ELASTIC MODULUS I - FULLY FLOODED CONJUNCTION | 5. Report Date August 1977 | 6. Performing Organization Code |
| 7. Author(s) Bernard J. Hamrock, Lewis Research Center; and Duncan Dowson, Leeds University, Leeds, England | 8. Performing Organization Report No. E-9216 | 10. Work Unit No. |
| 9. Performing Organization Name and Address National Aeronautics and Space Administration Lewis Research Center Cleveland, Ohio 44135 | 11. Contract or Grant No. | 13. Type of Report and Period Covered Technical Note |
| 12. Sponsoring Agency Name and Address National Aeronautics and Space Administration Washington, D.C. 20546 | 14. Sponsoring Agency Code | |
| 15. Supplementary Notes | | |
| 16. Abstract Our earlier studies of elastohydrodynamic lubrication of conjunctions of elliptical form are applied to the particular and interesting situation exhibited by materials of low elastic modulus. By modifying the procedures we outlined in an earlier publication, the influence of the ellipticity parameter k and the dimensionless speed U , load W , and material G parameters on minimum film thickness for these materials has been investigated. The ellipticity parameter was varied from 1 (a ball-on-plate configuration) to 12 (a configuration approaching a line contact). The dimensionless speed and load parameters were varied by 1 order of magnitude. Seventeen different cases were used to generate the following minimum- and central-film-thickness relations: $\tilde{H}_{\min} = 7.43(1 - 0.85 e^{-0.31k})U^{0.65}W^{-0.21}$; and $\tilde{H}_c = 7.32(1 - 0.72 e^{-0.28k})U^{0.64}W^{-0.22}$. Contour plots are presented that illustrate in detail the pressure distribution and film thickness in the conjunction. | | |
| 17. Key Words (Suggested by Author(s)) Elastohydrodynamic lubrication; Materials of low elastic modulus; Seals; Human joints; Elastomeric-material machine elements | 18. Distribution Statement Unclassified - unlimited STAR Category 37 | |
| 19. Security Classif. (of this report) Unclassified | 20. Security Classif. (of this page) Unclassified | 21. No. of Pages 29 |
| | | 22. Price* A03 |



ELASTOHYDRODYNAMIC LUBRICATION OF ELLIPTICAL CONTACTS FOR
MATERIALS OF LOW ELASTIC MODULUS
I - FULLY FLOODED CONJUNCTION

by Bernard J. Hamrock and Duncan Dowson*

Lewis Research Center

SUMMARY

Our earlier studies of elastohydrodynamic lubrication of conjunctions of elliptical form are applied to the particular and interesting situation exhibited by materials of low elastic modulus. By modifying the procedures we outlined in an earlier publication, the influence of the ellipticity parameter k and the dimensionless speed U , load W , and material G parameters on minimum film thickness for these materials has been investigated. The ellipticity parameter was varied from 1 (a ball-on-plate configuration) to 12 (a configuration approaching a line contact). The dimensionless speed and load parameters were varied by 1 order of magnitude. Seventeen different cases were used to generate the following minimum- and central-film-thickness relations:

$$\tilde{H}_{\min} = 7.43(1 - 0.85 e^{-0.31k})U^{0.65}W^{-0.21}$$

$$\tilde{H}_c = 7.32(1 - 0.72 e^{-0.28k})U^{0.64}W^{-0.22}$$

Contour plots are presented that illustrate in detail the pressure distribution and film thickness in the conjunction.

* Professor of Mechanical Engineering, Leeds University, Leeds, England.

INTRODUCTION

Only in recent years has the complete numerical solution of the isothermal elastohydrodynamic lubrication (EHL) of elliptical contacts successfully emerged. The analysis requires the simultaneous solution of the elasticity and Reynolds equations. The authors' approach to the theoretical solution has been presented in two previous publications (refs. 1 and 2). The first of these publications (ref. 1) presents an elasticity model in which the conjunction is divided into equal rectangular regions with a uniform pressure applied over each region. The second (ref. 2) gives a complete approach to the solution of the elastohydrodynamic lubrication problem for point contacts.

The most important practical aspect of the EHL point-contact theory (ref. 2) is the determination of the minimum film thickness within the contact. That is, the prediction of a film of adequate thickness is extremely important for the successful operation of machine elements in which these thin, continuous, fluid films occur. In a recent paper by the authors (ref. 3) the fully flooded results obtained from the theory given in references 1 and 2 were presented. A fully flooded condition is said to exist when the inlet distance of the conjunction ceases to influence in any significant way the minimum film thickness. In reference 3 the influence of the ellipticity parameter and the dimensionless speed, load, and material parameters on minimum film thickness was investigated. Thirty-four different cases were used in obtaining the fully flooded minimum-film-thickness formula.

In reference 4 the basic theory developed in references 1 and 2 was used to study the effect of lubricant starvation on the pressure and film thickness within the conjunction. A simple expression for the dimensionless inlet boundary distance was obtained. This inlet boundary distance defines whether a fully flooded or a starved condition exists in the contact. Fifteen cases, in addition to three presented in reference 3, were used to obtain simple expressions for the minimum and central film thicknesses in a starved conjunction.

The work presented in references 1 to 4 related to a material of high elastic modulus (e. g. , steel). The work presented in the present report is for a material of low elastic modulus (e. g. , nitrile rubber). For such materials the distortions are large even with light loads. Another feature of the EHL of low-elastic-modulus materials is the negligible effect of pressure on the viscosity of the lubricating fluid. Engineering applications in which elastohydrodynamic lubrication is important for low-elastic-modulus materials include seals, human joints, tires, and elastomeric-material machine elements.

The problem of line contacts, where side leakage of the fluid is ignored, has been solved theoretically for low-elastic-modulus materials by Herrebrugh (ref. 5), Dowson and Swales (ref. 6), and Baglin and Archard (ref. 7). The solutions of references 5

and 6 were obtained numerically and are based on simultaneous solutions of the hydrodynamic and elasticity equations; the analytical solution of reference 7 relied on the assumption of a simplified form for the film shape in the contact region. Biswas and Snidle (ref. 8) used the approach of reference 7 to solve the point-contact (ball on plate) situation. The present work represents, to the best of the authors' knowledge, the first attempt at a complete numerical solution of the problem of isothermal elastohydrodynamic lubrication of elliptical contacts for low-elastic-modulus materials. In this report, no assumptions are made as to the pressure or film thickness within the contact, and compressibility and viscous effects are considered.

SYMBOLS

| | |
|------------------|--|
| a | semimajor axis of contact ellipse |
| b | semiminor axis of contact ellipse |
| D_1 | $\left(\frac{\tilde{H}_{\min} - H_{\min}}{H_{\min}} \right) 100$ |
| D_2 | $\left(\frac{\tilde{H}_c - H_c}{H_c} \right) 100$ |
| E | modulus of elasticity |
| E' | $\frac{2}{\left(\frac{1 - \nu_A^2}{E_A} + \frac{1 - \nu_B^2}{E_B} \right)}$ |
| F | normal applied load |
| G | dimensionless material parameter, E'/p_{iv} , as |
| H | dimensionless film thickness, h/R_x |
| H_c | dimensionless central film thickness obtained from EHL elliptical contact theory |
| \tilde{H}_c | dimensionless central film thickness obtained from least-squares fit of data |
| H_{\min} | dimensionless minimum film thickness obtained from EHL elliptical contact theory |
| \bar{H}_{\min} | dimensionless film thickness - speed parameter, $H_{\min} U^{-0.5}$ |

| | |
|------------------------------|---|
| $\{\bar{H}_{\min}\}_B$ | dimensionless film thickness - speed parameter from ref. 8 |
| $\{\bar{H}_{\min}\}_H$ | dimensionless film thickness - speed parameter from present analysis |
| $\{\bar{H}_{\min}\}_J$ | dimensionless film thickness - speed parameter from unpublished data by W. E. Jamison of Clemson University |
| $\{\bar{\bar{H}}_{\min}\}_K$ | dimensionless film thickness - speed parameter from ref. 9 |
| \hat{H}_{\min} | dimensionless minimum film thickness obtained from EHL elliptical contact theory for materials of <u>high</u> elastic modulus (ref. 3) |
| \tilde{H}_{\min} | dimensionless minimum film thickness obtained from least-squares fit of data |
| $H_{\min, L}$ | dimensionless minimum film thickness for line contact |
| H_o | constant, initially estimated |
| h | film thickness |
| k | ellipticity parameter, a/b |
| M_P | dimensionless load-speed parameter, $WU^{-0.75}$ |
| P | dimensionless pressure, p/E' |
| P_D | dimensionless pressure difference |
| P_{Hz} | dimensionless Hertzian pressure |
| p | pressure |
| $p_{iv, as}$ | asymptotic isoviscous pressure |
| R | effective radius |
| r | radius of curvature |
| S | natural separation of elliptical solids |
| U | dimensionless speed parameter, $u\eta_0/E'R_x$ |
| u | mean surface velocity in x-direction, $\frac{1}{2}(u_A + u_B)$ |
| W | dimensionless load parameter, $F/E'R_x^2$ |
| w_{Hz} | elastic deformation due to Hertzian pressure distribution |
| $w _{P_D}$ | elastic deformation due to pressure difference, from eq. (2) |

x, X, \bar{X}
 y, Y, \bar{Y} } coordinate systems defined in report

α pressure-viscosity coefficient

$\bar{\eta}$ dimensionless viscosity

η_0 atmospheric viscosity

ν Poisson's ratio

ρ lubricant density

$\bar{\rho}$ dimensionless density, ρ/ρ_0

ρ_0 atmospheric density

Subscripts:

A solid A

B solid B

x, y coordinate system defined in report

THEORETICAL FORMULATION

The basic theory developed in reference 2 is used here with some minor modifications. It was discovered that numerical convergence was considerably better if the dimensionless pressure was written as

$$P = P_{Hz} + P_D \quad (1)$$

P_{Hz} dimensionless Hertzian pressure

P_D dimensionless pressure difference

By making use of equation (1), the relevant Reynolds equation can be written as

$$\frac{\partial}{\partial X} \left(\frac{\bar{\rho} H^3}{\bar{\eta}} \frac{\partial P_D}{\partial X} \right) + \frac{1}{k^2} \frac{\partial}{\partial Y} \left(\frac{\bar{\rho} H^3}{\bar{\eta}} \frac{\partial P_D}{\partial Y} \right) + \frac{\partial}{\partial X} \left(\frac{\bar{\rho} H^3}{\bar{\eta}} \frac{\partial P_{Hz}}{\partial X} \right) + \frac{1}{k^2} \frac{\partial}{\partial Y} \left(\frac{\bar{\rho} H^3}{\bar{\eta}} \frac{\partial P_{Hz}}{\partial Y} \right) = 12U \left(\frac{b}{R_x} \right) \frac{\partial (\bar{\rho} H)}{\partial X} \quad (2)$$

where $k = a/b$ is the ellipticity parameter. Since the Hertzian pressure is known, the solution of the Reynolds equation involves solving for P_D . In equation (2), compressibility and viscous effects are considered even though it was mentioned in the INTRODUCTION that the effect of pressure on viscosity and density is negligible.

The equation for the dimensionless film thickness is written as

$$H = H_0 + \frac{(S + w_{Hz} + w|_{P_D})}{R_x} \quad (3)$$

H_0 constant (initially guessed)

S natural separation of elliptical solids

w_{Hz} elastic deformation due to Hertzian pressure distributions

$w|_{P_D}$ elastic deformation due to pressure difference obtained from eq. (2)

The evaluation of the elastic deformation is exactly that used in references 1 and 2.

The nodal structure used for obtaining all the results is shown in figure 1. It should be noted from this figure that, because of the dimensionless representation of the coordinates, the actual Hertzian contact ellipse becomes a circle regardless of the value of k . The nodal structure shown in figure 1 was arrived at after much exploration in which the number of nodes in the semimajor and semiminor axes, as well as the distance from the center of the contact to the edges of the computing zone, was varied.

DIMENSIONLESS GROUPING

The same dimensionless grouping of parameters used in the analysis of elastohydrodynamic lubrication of high-elastic-modulus materials (ref. 3) is used herein:

Dimensionless film thickness:

$$H = \frac{h}{R_x} \quad (4)$$

Ellipticity parameter:

$$k = \frac{a}{b} \quad (5)$$

Dimensionless speed parameter:

$$U = \frac{\eta_0 u}{E' R_x} \quad (6)$$

Dimensionless load parameter:

$$W = \frac{F}{E' R_x^2} \quad (7)$$

Dimensionless material parameter:

$$G = \frac{E'}{p_{iv, as}} \quad (8)$$

where $p_{iv, as}$ is the asymptotic isoviscous pressure obtained from Roelands (ref. 10). The asymptotic isoviscous pressure can be approximated by the inverse of the pressure-viscosity coefficient, $p_{iv, as} \approx (1/\alpha)$.

The dimensionless film thickness can be written as

$$H = f(k, U, W, G) \quad (9)$$

The most important practical aspect of the elastohydrodynamic lubrication elliptical contact theory is the determination of the minimum film thickness within the conjunction. Therefore, in the fully flooded results presented herein, the dimensionless parameters k , U , W , and G were varied, and the effect upon minimum film thickness studied. Care was taken to ensure that all results were in the elastic region.

EFFECT OF ELLIPTICITY OF ELASTIC CONJUNCTION

The ellipticity parameter is a function of the radii of curvature of the solids only (r_{Ax} , r_{Bx} , r_{Ay} , and r_{By}). The radii of curvature in the x-direction for both solids A and B are used in defining the dimensionless speed and load parameters. Therefore, only the radius of curvature of solid B in the y-direction was changed in varying k from 1 (a ball-on-plate configuration) to 12 (a configuration approaching a line contact). In doing this, the dimensionless speed, load, and material parameters were held constant at

$$\left. \begin{aligned} U &= 0.1028 \times 10^{-7} \\ W &= 0.4405 \times 10^{-3} \\ G &= 0.4276 \end{aligned} \right\} \quad (10)$$

Table I gives seven values of the ellipticity parameter and the corresponding minimum film thickness as obtained from the EHL elliptical contact theory. Having these seven pairs of data, the object was to determine an equation that would describe how the ellipticity parameter affects the minimum film thickness. The general form of this equation can be written as

$$\left(1 - \frac{H_{\min}}{H_{\min, L}} \right) = A e^{Bk} \quad (11)$$

A least-squares exponential curve fit to the seven pairs of data points

$$k_i, \left[\left(1 - \frac{H_{\min}}{H_{\min, L}} \right)_i \right] \quad i = 1, \dots, 7$$

was used in obtaining values for A and B in equation (11). Besides a least-squares fit, a coefficient of determination r^2 was obtained. The value of r^2 reflects the fit of the data to the resulting equation: 1 being a perfect fit, and zero the worst possible fit. The minimum film thickness for a line contact $H_{\min, L}$ used in equation (11) was determined by finding the $H_{\min, L}$ that gives a coefficient of determination closest to 1. This value of $H_{\min, L}$ turned out to be 240.0×10^{-6} , with a corresponding coefficient of determination of 0.9908, which is an excellent fit. Furthermore, the values of A and B in equation (11), as obtained from the least-squares fit, are

$$A = 0.8488 \approx 0.85 \quad (12)$$

$$B = -0.3115 \approx -0.31 \quad (13)$$

From equations (11) to (13), the following equation can be written, which shows the effect of k on \tilde{H}_{\min} :

$$\tilde{H}_{\min} \propto (1 - 0.85 e^{-0.31k}) \quad (14)$$

Figure 2 shows the variation of the ratio $H_{\min}/H_{\min,L}$ with k for the EHL high-elastic-modulus analysis (ref. 3) and the EHL low-elastic-modulus analysis (present results). If we assume that the minimum film thickness obtained from the EHL elliptical analysis can only be obtained to an accuracy of 3 percent, we find a limiting solution for line contact being approached for a k of 5 for the EHL high-elastic-modulus analysis and for a k of 11 for the EHL low-elastic-modulus analysis.

INFLUENCE OF SPEED

Changing only the surface velocity in the x -direction u causes the dimensionless speed parameter U to change while the other dimensionless parameters (k , W , and G) remain constant. The values at which these dimensionless parameters were held constant in the calculations were

$$\left. \begin{aligned} W &= 0.4405 \times 10^{-3} \\ k &= 6 \\ G &= 0.4276 \end{aligned} \right\} \quad (15)$$

Table I also gives the dimensionless speed parameter and the corresponding dimensionless minimum film thickness as obtained from the EHL elliptical contact theory. There are five different values of the dimensionless speed parameter covering 1 order of magnitude. Having these five pairs of data, the objective was to determine an equation that would describe how the speed affects the minimum film thickness. The general form of this equation can be written as

$$H_{\min} = IU^J \quad (16)$$

By applying a least-squares power fit to the five pairs of data, $(U_i, H_{\min,i})$, where $i = 1, \dots, 5$, the values of I and J were found to be

$$I = 32.48 \quad (17)$$

$$J = 0.6505 \approx 0.65 \quad (18)$$

The coefficient of determination r^2 for these results was excellent at 0.9997. From equations (16) and (18) the effect of dimensionless speed on dimensionless minimum film thickness can be written as

$$\tilde{H}_{\min} \propto U^{0.65} \quad (19)$$

Figure 3 gives contour plots of dimensionless pressure for two extreme values of U , 0.05139×10^{-7} and 0.5139×10^{-7} . In these and all contour plots to be presented, the + symbol indicates the center of the Hertzian contact. Because of the dimensionless representation of the X and Y coordinates, the actual Hertzian contact ellipse becomes a circle regardless of the value of k . The Hertzian contact circle is shown in each figure by asterisks. At the top of each figure the contour labels and the corresponding values of dimensionless pressure are given. The inlet region is to the left, and the exit region to the right.

The pressure contours shown in figure 3 are nearly circular, or Hertzian. In figure 3(b), the high-speed case, the inlet pressure was higher than in the low-speed case shown in figure 3(a). Inside the contact the contour values of the dimensionless pressure were higher for the low-speed case (fig. 3(a)). The pressure spikes found when dealing with materials of high elastic modulus (ref. 3) were not in evidence in these solutions for low-elastic-modulus materials. The lack of a pressure spike is due to the lack of viscous effects of the fluid in the contact for low-elastic-modulus materials. This in turn is due to the fact that considerably less pressure is generated in a contact with low-elastic-modulus materials than in a contact with high-elastic-modulus materials.

Figure 4 shows contour plots of dimensionless film thickness for two values of U , 0.05139×10^{-7} and 0.5139×10^{-7} . Figure 4(a) shows two regions of minimum film thickness, close to the Hertzian circle and off to the side. Figure 4(b) shows one region of minimum film thickness, between the center of the contact and the Hertzian circle.

Figure 5 shows the variation of pressure and film thickness on the X -axis near the midplane of the conjunction for the same two values of U . For all the solutions for various speeds, the values of the dimensionless load, material, and ellipticity parameters were held fixed as described in equation (15). In figure 5 the pressure in the inlet region is higher for the higher speed ($U = 0.5139 \times 10^{-7}$) profile. It should be noted that these slight changes in pressure that occur when the speed is increased by 1 order of magnitude result in a significant change in film thickness, as indicated by equation (19).

This illustrates most clearly the dominant effect of the dimensionless speed parameter on the minimum film thickness in elastohydrodynamic contacts for low-elastic-modulus materials. Similar results were found for high-elastic-modulus materials (ref. 3).

INFLUENCE OF LOAD

Changing only the normal applied load F in equation (7) causes the dimensionless load parameter W to change while the other dimensionless parameters (k , U , and G) remain constant. The values at which these parameters were held constant were

$$\left. \begin{aligned} U &= 0.1028 \times 10^{-7} \\ k &= 6 \\ G &= 0.4276 \end{aligned} \right\} \quad (20)$$

The load results presented in table I give the dimensionless load parameter and the corresponding minimum film thickness as obtained from the EHL elliptical contact theory. There are six different values of dimensionless load parameter covering 1 order of magnitude. Having these six pairs of data, the objective was to determine an equation that would describe how the dimensionless load affects the minimum film thickness. The general form of this equation can be written as

$$C = KW^L \quad (21)$$

where

$$C = \frac{H_{\min}}{(1 - 0.85 e^{-0.31k})U^{0.65}} \quad (22)$$

In equation (22) the exponents are rounded off to two significant figures so that any error could be absorbed in K , given in equation (21). By applying a least-squares power fit to the six pairs of data $[(W_i, C_i), i = 1, \dots, 6]$, the values of K and L were found to be

$$K = 6.507 \quad (23)$$

$$L = -0.2075 \approx -0.21 \quad (24)$$

The coefficient of determination r^2 for these results was 0.9985, which is excellent. From equations (21), (22), and (24), the effect of load on minimum film thickness can be written as

$$\tilde{H}_{\min} \propto W^{-0.21} \quad (25)$$

Figure 6 gives contour plots of dimensionless pressure for the two extreme values of W that were investigated, 0.2202×10^{-3} and 2.202×10^{-3} . Again the pressure contours were nearly circular, or Hertzian. The contour values were considerably higher for the high-load case (fig. 6(b)).

Contour plots of dimensionless film thickness for the same two values of W are shown in figure 7. In figure 7(a), for the low-load case ($W = 0.2202 \times 10^{-3}$), the minimum film thickness occurred directly behind the center of the contact; in figure 7(b), for the high-load case ($W = 2.202 \times 10^{-3}$), the minimum film thickness also occurred directly behind the center of the contact but closer to the Hertzian circle. The two C contours in figure 7(b) indicate a slight increase in film thickness before the minimum-film-thickness region is reached.

The variation of pressure and film thickness in the X-direction along a line close to the midplane of the conjunction is shown in figure 8 for two values of W . The values of U , G , and k were held fixed as described by equation (20) for all computations at various loads. In this figure, for a 1-order-of-magnitude change in the dimensionless load parameter, there is a considerable change in the pressure profile but not such a significant change in the film thickness profile.

MINIMUM-FILM-THICKNESS FORMULA

The proportionality expressions (14), (19), and (25) established how the minimum film thickness varied with the ellipticity, speed, and load parameters, respectively. This enabled a composite minimum-film-thickness formula for a fully flooded, isothermal, elastohydrodynamic elliptical contact for low-elastic modulus materials to be written as

$$\tilde{H}_{\min} = 7.43(1 - 0.85 e^{-0.31k})U^{0.65}W^{-0.21} \quad (26)$$

In equation (26) the constant 7.43 is different from that given in equation (23) to account for rounding off the load-parameter exponent.

Table I gives the values for the minimum film thickness obtained from the least-squares fit as defined by equation (26). The percentage difference between the minimum film thickness obtained from the EHL elliptical contact theory H_{\min} and the minimum film thickness obtained from the least-squares fit equation \tilde{H}_{\min} is expressed as

$$D_1 = \left(\frac{\tilde{H}_{\min} - H_{\min}}{H_{\min}} \right) 100 \quad (27)$$

In table I the values of D_1 are within the range -8 and +3.

It is sometimes more convenient to express the side-leakage factor in equation (26) in terms of the curvature ratio R_y/R_x instead of the ellipticity parameter through the following relation:

$$k = 1.03 \left(\frac{R_y}{R_x} \right)^{0.64} \quad (28)$$

where

$$\frac{1}{R_y} = \frac{1}{r_{Ay}} + \frac{1}{r_{By}} \quad (29)$$

$$\frac{1}{R_x} = \frac{1}{r_{Ax}} + \frac{1}{r_{Bx}} \quad (30)$$

Using equation (28) avoids the need to evaluate elliptic integrals of the first and second kinds in the determination of k . The minimum film thickness can thus be derived directly from a knowledge of the curvature of the contacting bodies (r_{Ax} , r_{Bx} , r_{Ay} , and r_{By}).

It is interesting to compare the equation for materials of low elastic modulus (eq. (26)) with the corresponding equation generated in reference 3 for materials of high elastic modulus

$$\hat{H}_{\min} = 3.63 U^{0.68} G^{0.49} W^{-0.073} (1 - e^{-0.68k}) \quad (31)$$

The powers of U in equations (26) and (31) are quite similar, but the power of W is much more significant for low-elastic-modulus materials. The expression showing the effect of the ellipticity parameter is of exponential form in both equations, but with quite different constants.

A major difference in equations (26) and (31) is the absence of a material parameter in the expression for the minimum film thickness for low-elastic-modulus materials. There are two reasons for this. One is the negligible effect of pressure on the viscosity of the lubricating fluid for low-elastic-modulus materials. The other is the way in which the role of elasticity is simply and automatically incorporated in the prediction of conjunction behavior through an increase in the size of the Hertzian contact zone corresponding to changes in load. As a check on the validity of this, case 9 of table I was repeated with the material changed from nitrile rubber to silicone rubber. This is recorded as case 17 (table I). As can be seen from equations (6) to (8), when the material (as expressed by E') is changed, not only does the material parameter change, but so do the dimensionless speed and load parameters. Only the ellipticity parameter can be held fixed. From table I, case 17, we find that the minimum film thickness from the EHL elliptical contact theory was 181.8×10^{-6} . The minimum film thickness from the least-squares fit (eq. (26)) turned out to be 182.5×10^{-6} . This clearly indicates a lack of dependence of the minimum film thickness for low-elastic-modulus materials on the material parameter.

CENTRAL-FILM-THICKNESS FORMULA

There is interest in knowing the central film thickness, in addition to the minimum film thickness, in elastohydrodynamic contacts. The procedure used in obtaining the central film thickness was the same as that used in obtaining the minimum film thickness and is not repeated here. The central-film-thickness formula for low-elastic-modulus materials obtained from the results is

$$\tilde{H}_c = 7.32(1 - 0.72 e^{-0.28k}) U^{0.64} W^{-0.22} \quad (32)$$

Comparison of the central-film-thickness formula (eq. (32)) with the minimum-film-thickness formula (eq. (26)) reveals only slight differences.

Table II gives the 16 different cases used to obtain equation (32), as well as case 17, which is a check on equation (32). In this table, H_c corresponds to the central film thickness obtained from the EHL elliptical contact theory and \tilde{H}_c corresponds to the central film thickness obtained from equation (32). The percentage difference between these two values is given by D_2 and is written as

$$D_2 = \left(\frac{\tilde{H}_c - H_c}{H_c} \right) 100 \quad (33)$$

In table II the values of D_2 are within the range -11 to +23.

The ratio of minimum to central film thickness evident in the computed values ranged from 70 to 83 percent, the average being 77 percent.

Comparison of Different Investigators' Results

To evaluate the dimensionless minimum-film-thickness equation (eq. (26)) developed in this report, a comparison was made between it, the numerical solution obtained by Biswas and Snidle (ref. 8), and the recent experimental findings of Jamison (unpublished data). Both are applicable only for $k = 1$.

From reference 8 the dimensionless minimum film thickness can be written as

$$\left\{ \bar{H}_{\min} \right\}_B = 1.96 M_P^{-0.11} \quad (34)$$

where

$$\bar{H}_{\min} = H_{\min} U^{-0.5} \quad (35)$$

$$M_P = WU^{-0.75} \quad (36)$$

The dimensionless groups given in equations (35) and (36) were first used by Moes and Bosma (ref. 11).

The central-film-thickness equation obtained from the experimental results of Jamison can be written as

$$\left\{ \bar{H}_c \right\}_J = 2.4 M_P^{-0.075} \quad (37)$$

where

$$\bar{H}_c = H_c U^{-0.5} \quad (38)$$

Modifying equation (37) to provide a minimum-film-thickness equation by using the assumption that $\left\{ \bar{H}_{\min} \right\}_J = 0.78 \left\{ H_c \right\}_J$ yields

$$\left\{ \bar{H}_{\min} \right\}_J = 1.87 M_P^{-0.075} \quad (39)$$

Equations (34) and (39) are valid only for $k = 1$.

By making use of equations (35), (36), and table I equation (26) can be written as

$$\left\{ \bar{H}_{\min} \right\}_H = 8.53(1 - 0.85 e^{-0.31k}) M_P^{-0.21} \quad (40)$$

Therefore, for $k = 1$, equation (40) reduces to

$$\left\{ \bar{H}_{\min} \Big|_{k=1} \right\}_H = 3.21 M_P^{-0.21} \quad (41)$$

Note the larger negative exponent in equation (41) than in either equations (34) or (39).

Figure 9 compares the different investigators' results from equations (34), (39), and (41). The three equations seem to agree quite well with each other. The present report's results are equivalent to the Biswas and Snidle theoretical results (ref. 8) at $M_P = 100$ and the Jamison experimental results at $M_P = 45$. Therefore, even though the exponent on M_P for the present results is larger than those obtained in reference 8 and by Jamison, the agreement is quite good for $k = 1$. Also shown in figure 9 is the rigid isoviscous solution obtained from Kapitza (ref. 9).

Figure 10 uses equation (40) to show the effect of the dimensionless parameter M_P on the dimensionless minimum film thickness for six values of the ellipticity parameter. As k increases, less change occurs in the dimensionless minimum film thickness. From this figure the dimensionless minimum film thickness can easily be obtained for known values of k and M_P .

Similarly, the equation for the dimensionless central film thickness can be written as

$$\left\{ \bar{H}_c \right\}_H = 11.61(1 - 0.72 e^{-0.28k}) M_P^{-0.22} \quad (42)$$

Figure 11 uses equation (42) to show the effect of the dimensionless parameter M_P on the dimensionless central film thickness for six values of k .

CONCLUDING REMARKS

By modifying the procedures outlined by the authors in an earlier publication, the influence of the ellipticity parameter k and the dimensionless speed U , load W , and material G parameters on minimum film thickness for low-elastic-modulus materials has been investigated. The ellipticity parameter was varied from 1 (a ball-on-plate configuration) to 12 (a configuration approaching a line contact). The dimensionless speed and load parameters were varied by 1 order of magnitude. Seventeen different cases were used to generate the minimum- and central-film-thickness relations:

$$\tilde{H}_{\min} = 7.43(1 - 0.85 e^{-0.31k})U^{0.65}W^{-0.21}$$

$$\tilde{H}_c = 7.32(1 - 0.72 e^{-0.28k})U^{0.64}W^{-0.22}$$

Contour plots have been presented that show in detail the pressure distribution and the film thickness in the conjunction.

The present report presents for the first time a complete theoretical film-thickness solution for the problem of isothermal elastohydrodynamic elliptical contacts for low-elastic-modulus materials operating under fully flooded conditions.

National Aeronautics and Space Administration,
Lewis Research Center,
Cleveland, Ohio, May 24, 1977,
505-04.

REFERENCES

1. Hamrock, Bernard J.; and Dowson, Duncan: Numerical Evaluation of the Surface Deformation of Elastic Solids Subjected to a Hertzian Contact Stress. NASA TN D-7774, 1974.

2. Hamrock, Bernard J.; and Dowson, Duncan: Isothermal Elastohydrodynamic Lubrication of Point Contacts. Part I - Theoretical Formulation. *J. Lubr. Technol.*, vol. 98, no. 2, Apr. 1976, pp. 223-229.
3. Hamrock, Bernard J.; and Dowson, Duncan: Isothermal Elastohydrodynamic Lubrication of Point Contacts. Part III - Fully Flooded Results. *J. Lubr. Technol.*, vol. 99, no. 2, Apr. 1977, pp. 264-276.
4. Hamrock, B. J.; and Dowson, D.: Isothermal Elastohydrodynamic Lubrication of Point Contacts. Part IV - Starvation Results. *J. Lubr. Technol.*, vol. 99, no. 1, Jan. 1977, pp. 15-23.
5. Herrebrugh, K.: Solving the Incompressible and Isothermal Problem in Elastohydrodynamic Lubrication Through an Integral Equation. *J. Lubr. Technol.*, vol. 90, no. 1, Jan. 1968, pp. 262-270.
6. Dowson, D.; and Swales, P. D.: The Development of Elastohydrodynamic Conditions in a Reciprocating Seal. *Proceedings of the Fourth International Conference on Fluid Sealing*, vol. 2, Paper 1, British Hydromechanics Research Association, 1969, pp. 1-9.
7. Baglin, K. P.; and Archard, J. F.: An Analytic Solution of the Elastohydrodynamic Lubrication of Materials of Low Elastic Modulus. *Symposium on Elastohydrodynamic Lubrication*, *Inst. Mech. Engrs.*, p. 13.
8. Biswas, S.; and Snidle, R. W.: Elastohydrodynamic Lubrication of Spherical Surfaces of Low Elastic Modulus. *J. Lubr. Technol.*, vol. 98, no. 4, Oct. 1976, pp. 524-529.
9. Kapitza, P. L.: Hydrodynamic Theory of Lubrication During Rolling. *Zh. Tekh. Fiz.*, vol. 25, no. 2, 1955, p. 747.
10. Roelands, C. J. A.: Correlational Aspects of the Viscosity-Temperature-Pressure Relationship of Lubricating Oils. *Druk V. R. B.*, Groningen, Netherlands, 1966.
11. Moes, H.; and Bosma, R.: Film Thickness and Traction in EHL at Point Contact. *Symposium on Elastohydrodynamic Lubrication*, *Inst. Mech. Engrs.*, 1972, p. 149.

TABLE I. - DATA SHOWING EFFECT OF ELLIPTICITY, LOAD, SPEED, AND MATERIAL PARAMETERS ON MINIMUM FILM THICKNESS

| Case | Ellipticity parameter, k | Dimensionless load parameter, W | Dimensionless speed parameter, U | Dimensionless material parameter, G | Minimum film thickness | | Difference between H_{\min} and \tilde{H}_{\min} , D_1 , percent | Results |
|------|--------------------------|---------------------------------|----------------------------------|-------------------------------------|---|---|--|---------------------|
| | | | | | Obtained from EHL elliptical contact theory, H_{\min} | Obtained from least-squares fit, \tilde{H}_{\min} | | |
| 1 | 1 | 0.4405×10^{-3} | 0.1028×10^{-7} | 0.4276 | 88.51×10^{-6} | 91.08×10^{-6} | +2.90 | } Ellipticity |
| 2 | 2 | ↓ | ↓ | ↓ | 142.5 | 131.2 | -7.93 | |
| 3 | 3 | ↓ | ↓ | ↓ | 170.4 | 160.8 | -5.63 | |
| 4 | 4 | ↓ | ↓ | ↓ | 186.7 | 182.4 | -2.30 | |
| 5 | 6 | ↓ | ↓ | ↓ | 206.2 | 209.8 | +1.75 | |
| 6 | 8 | ↓ | ↓ | ↓ | 219.7 | 224.6 | +2.23 | |
| 7 | 12 | ↓ | ↓ | ↓ | 235.2 | 236.0 | +0.34 | |
| 8 | 6 | ↓ | .05139 | ↓ | 131.8 | 133.7 | +1.44 | } Speed plus case 5 |
| 9 | ↓ | ↓ | .1542 | ↓ | 268.1 | 273.1 | +1.86 | |
| 10 | ↓ | ↓ | .2570 | ↓ | 381.6 | 380.7 | -0.24 | |
| 11 | ↓ | ↓ | .5139 | ↓ | 584.7 | 597.3 | +2.15 | |
| 12 | ↓ | .2202 | .1028 | ↓ | 241.8 | 242.7 | +0.37 | } Load plus case 5 |
| 13 | ↓ | .6607 | ↓ | ↓ | 190.7 | 192.7 | +1.05 | |
| 14 | ↓ | 1.101 | ↓ | ↓ | 170.5 | 173.1 | +1.52 | |
| 15 | ↓ | 1.542 | ↓ | ↓ | 160.4 | 161.3 | +0.56 | |
| 16 | ↓ | 2.202 | ↓ | ↓ | 149.8 | 149.7 | -0.07 | |
| 17 | ↓ | .1762 | .06169 | 1.069 | 181.8 | 182.5 | +0.39 | Material |

TABLE II. - DATA SHOWING EFFECT OF ELLIPTICITY, LOAD, SPEED, AND MATERIAL PARAMETERS ON CENTRAL FILM THICKNESS

| Case | Ellipticity parameter, k | Dimensionless load parameter, W | Dimensionless speed parameter, U | Dimensionless material parameter, G | Minimum film thickness | | Difference between H_c and \tilde{H}_c , D_2 , percent | Results |
|------|--------------------------|---------------------------------|----------------------------------|-------------------------------------|--|--|--|---------------------|
| | | | | | Obtained from EHL elliptical contact theory, H_c | Obtained from least squares fit, \tilde{H}_c | | |
| 1 | 1 | 0.4405×10^{-3} | 0.1028×10^{-7} | 0.4276 | 114.9×10^{-6} | 141.0×10^{-6} | +22.72 | } Ellipticity |
| 2 | 2 | ↓ | ↓ | ↓ | 204.2 | 182.2 | -10.77 | |
| 3 | 3 | ↓ | ↓ | ↓ | 217.2 | 213.2 | -1.84 | |
| 4 | 4 | ↓ | ↓ | ↓ | 253.1 | 236.7 | -6.48 | |
| 5 | 6 | ↓ | ↓ | ↓ | 265.0 | 267.9 | +1.09 | |
| 6 | 8 | ↓ | ↓ | ↓ | 288.8 | 285.7 | -1.07 | |
| 7 | 12 | ↓ | ↓ | ↓ | 307.1 | 301.7 | -1.76 | |
| 8 | 6 | ↓ | .05139 | ↓ | 171.7 | 171.9 | +1.12 | } Speed plus case 5 |
| 9 | ↓ | ↓ | .1542 | ↓ | 354.0 | 347.3 | -1.89 | |
| 10 | ↓ | ↓ | .2570 | ↓ | 498.7 | 481.5 | -3.45 | |
| 11 | ↓ | ↓ | .5139 | ↓ | 743.7 | 750.3 | +89 | |
| 12 | ↓ | .2202 | .1028 | ↓ | 316.3 | 312.0 | -1.36 | } Load plus case 5 |
| 13 | ↓ | .6607 | ↓ | ↓ | 235.1 | 245.0 | +4.21 | |
| 14 | ↓ | 1.101 | ↓ | ↓ | 221.5 | 219.0 | -1.13 | |
| 15 | ↓ | 1.542 | ↓ | ↓ | 192.6 | 203.4 | +5.61 | |
| 16 | ↓ | 2.202 | ↓ | ↓ | 196.6 | 188.0 | -4.37 | |
| 17 | ↓ | .1762 | .06169 | 1.069 | 237.4 | 236.3 | .46 | Material |

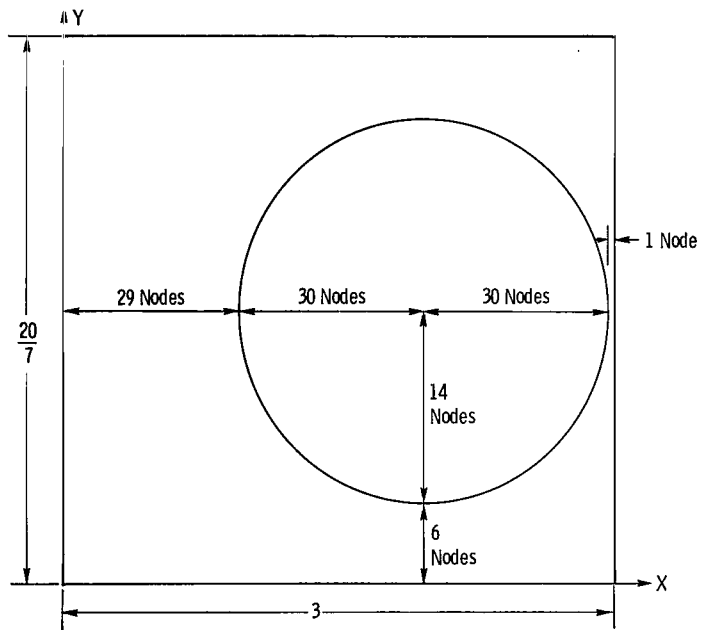


Figure 1. - Nodal structure used for numerical calculations.

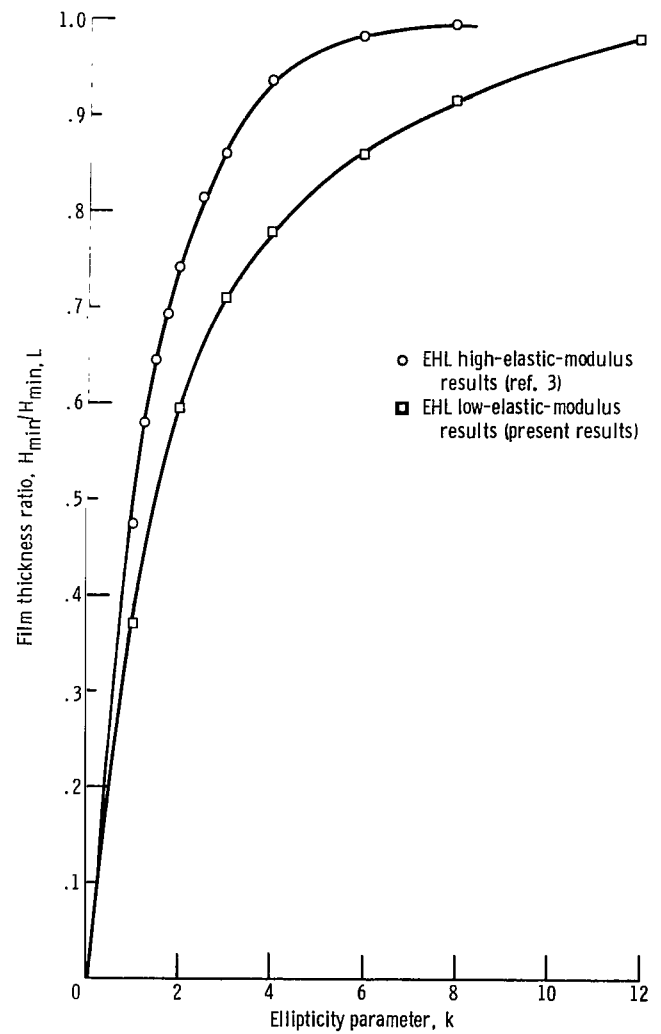


Figure 2. - Variation of ratio of dimensionless minimum film thickness to dimensionless minimum film thickness for a line contact with ellipticity parameter, for EHL high- and low-elastic-modulus analyses.

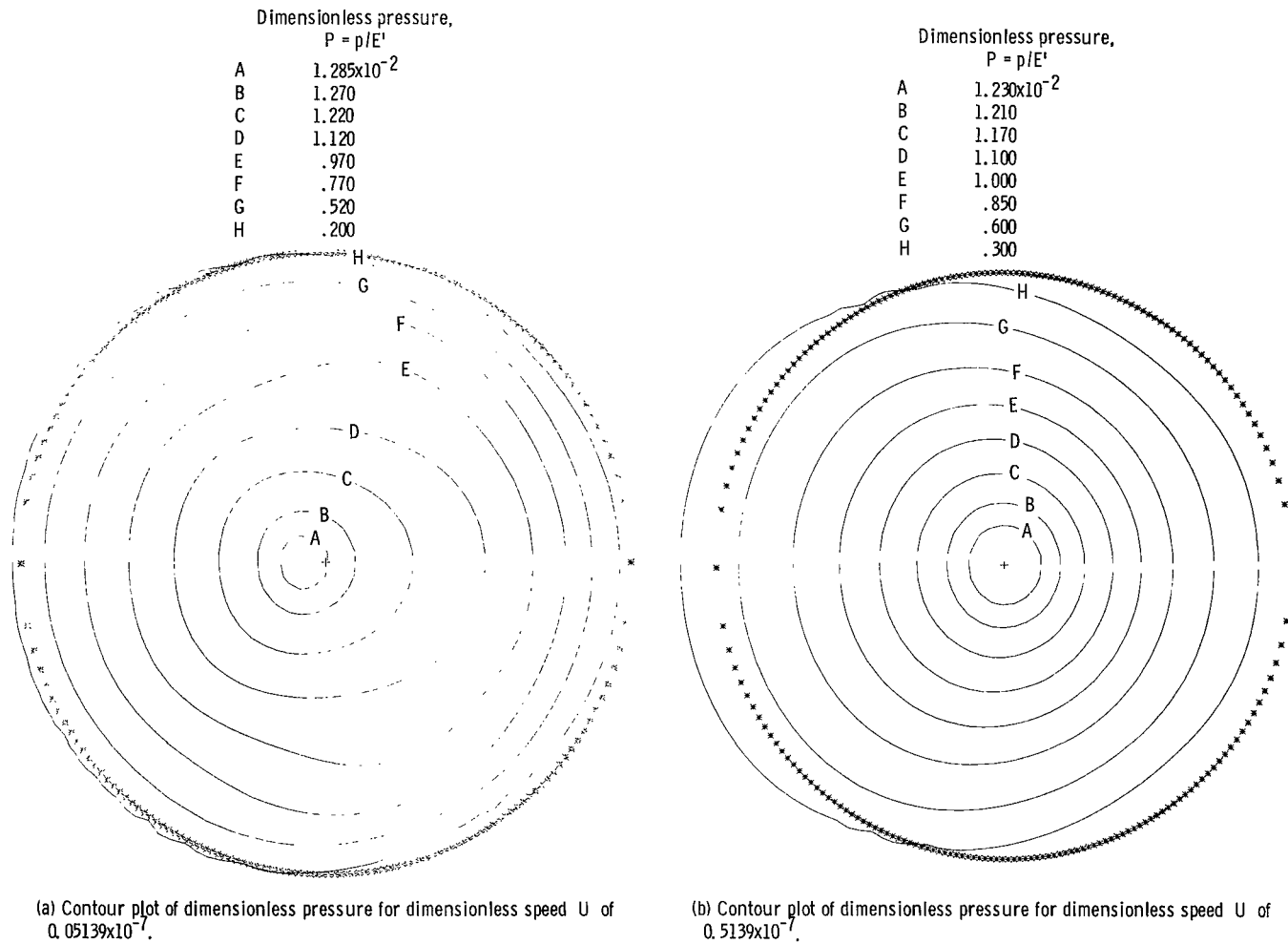
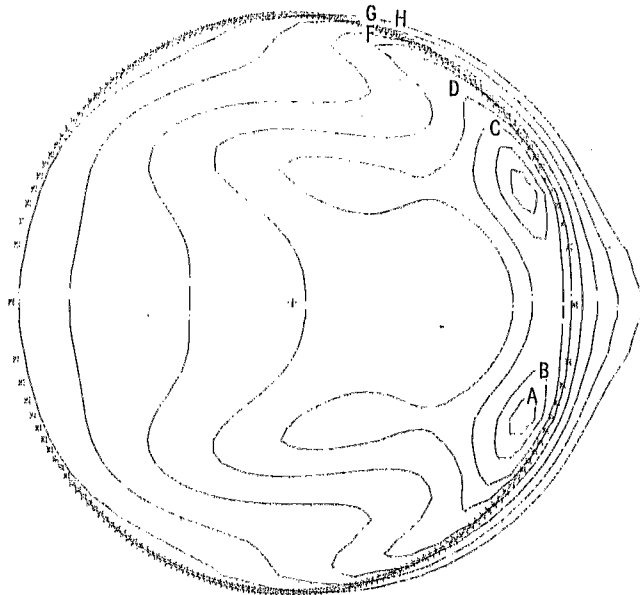


Figure 3. - Contour plots of dimensionless pressure for dimensionless speed parameters U of 0.05139×10^{-7} and 0.5139×10^{-7} . The dimensionless parameters k , W , and G are held constant as defined in equation (15).

Dimensionless
film thickness,
 $H = h/R_x$

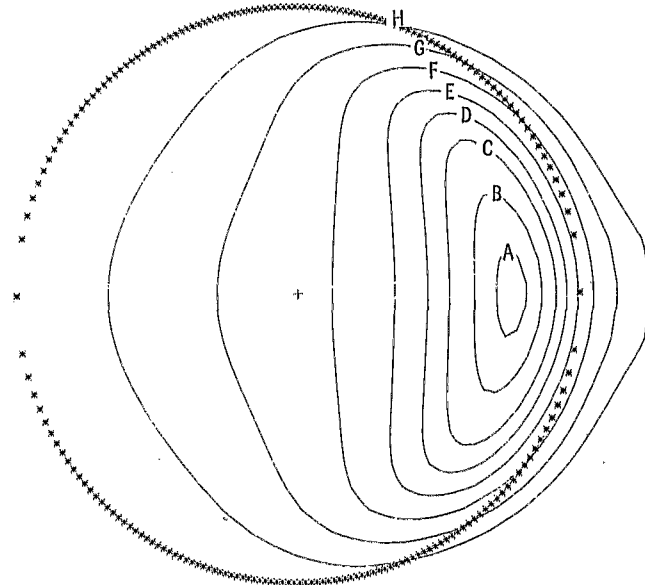
| | |
|---|-----------------------|
| A | 1.35×10^{-4} |
| B | 1.40 |
| C | 1.50 |
| D | 1.60 |
| E | 1.80 |
| F | 2.10 |
| G | 2.50 |
| H | 3.00 |



(a) Contour plot of dimensionless film thickness for dimensionless speed U of 0.05139×10^{-7} .

Dimensionless
film thickness,
 $H = h/R_x$

| | |
|---|-----------------------|
| A | 5.88×10^{-4} |
| B | 6.00 |
| C | 6.20 |
| D | 6.40 |
| E | 6.70 |
| F | 7.20 |
| G | 8.00 |
| H | 9.20 |



(b) Contour plot of dimensionless film thickness for dimensionless speed U of 0.5139×10^{-7} .

Figure 4. - Contour plots of dimensionless film thickness for dimensionless speed parameters U of 0.05139×10^{-7} and 0.5139×10^{-7} . The dimensionless parameters k , W , and G are held constant as defined in equation (15).

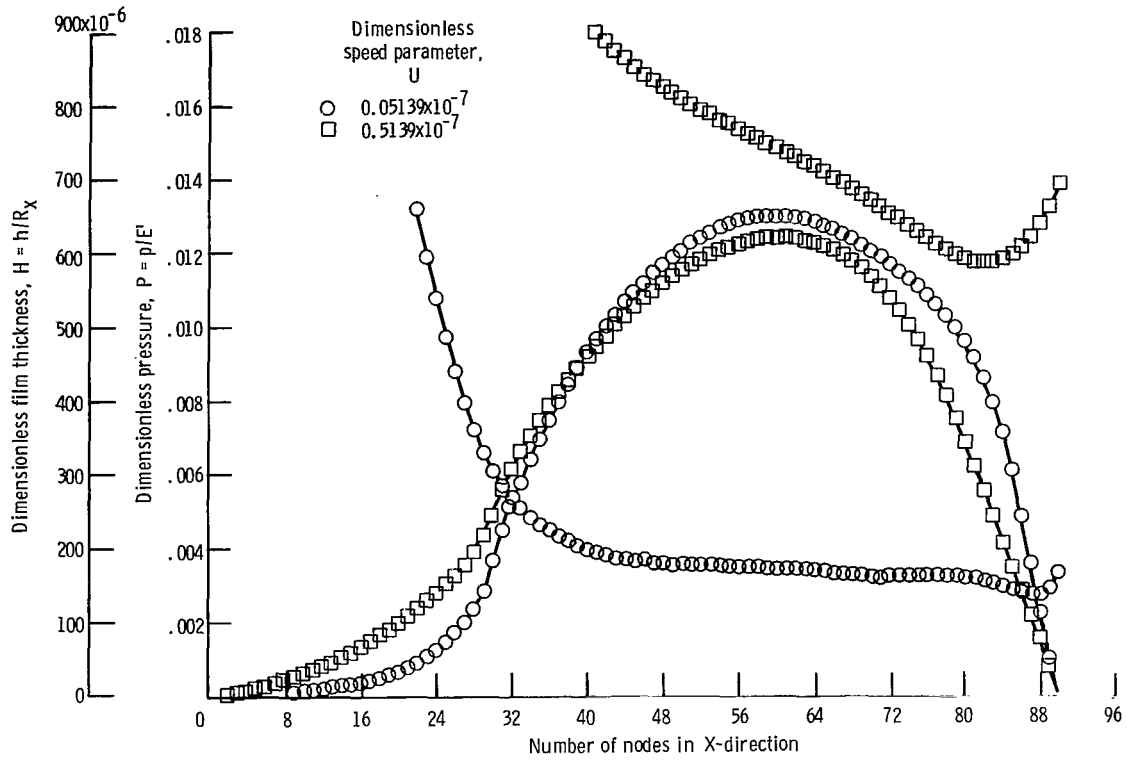
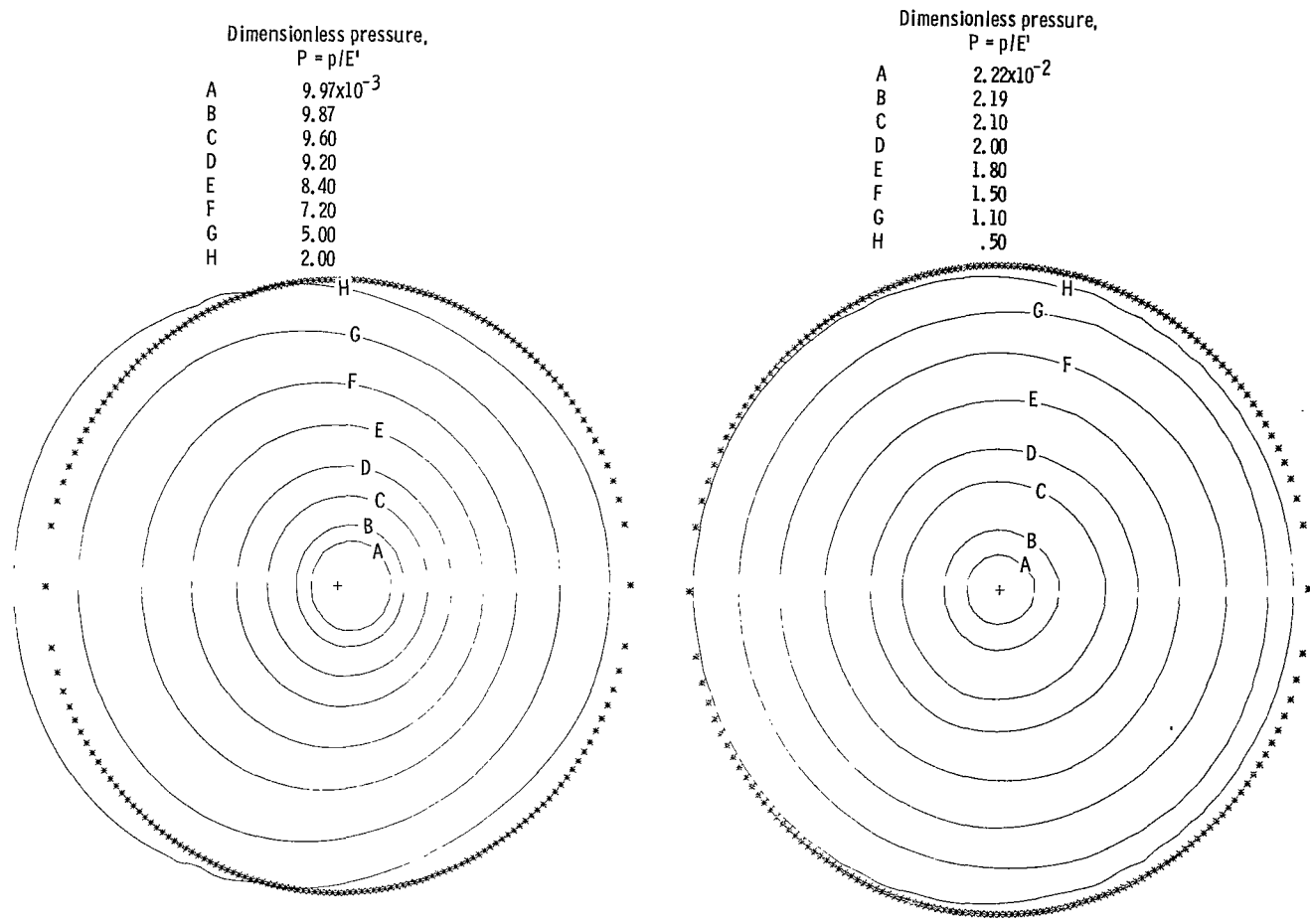


Figure 5. - Variation of dimensionless pressure and film thickness on X-axis for dimensionless speed parameters U of 0.05139×10^{-7} and 0.5139×10^{-7} . The value of Y is held fixed near axial center of contact.



(a) Contour plot of dimensionless pressure for dimensionless load W of 0.2202×10^{-3} .

(b) Contour plot of dimensionless pressure for dimensionless load W of 2.202×10^{-3} .

Figure 6. - Contour plots of dimensionless pressure for dimensionless loads W of 0.2202×10^{-3} and 2.202×10^{-3} . The dimensionless parameters k , U , and G are held constant as defined in equation (20).

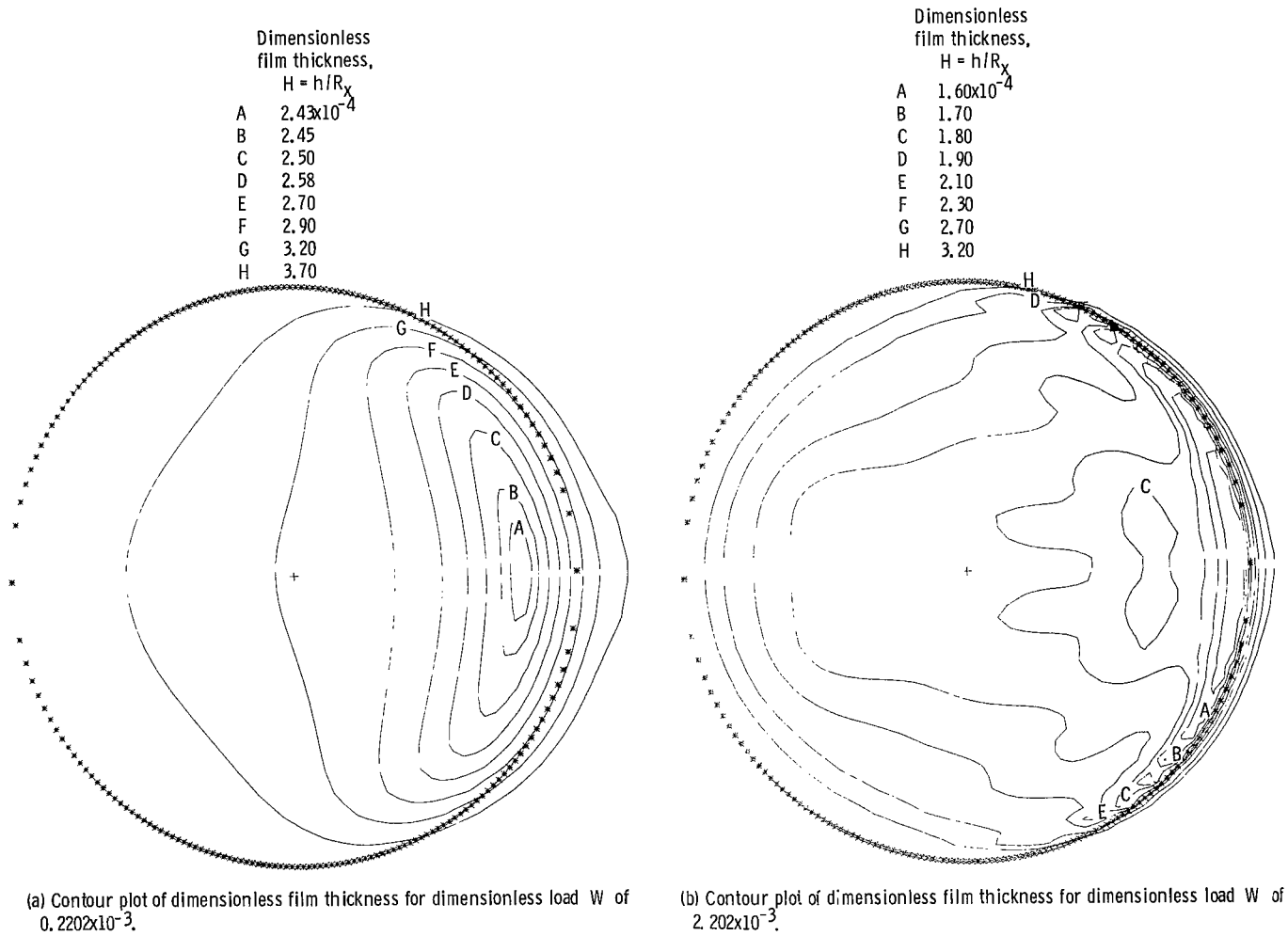


Figure 7. - Contour plots of dimensionless film thickness for dimensionless loads W of 0.2202×10^{-3} and 2.202×10^{-3} . The dimensionless parameters k , U , and G are held constant as defined in equation (20).

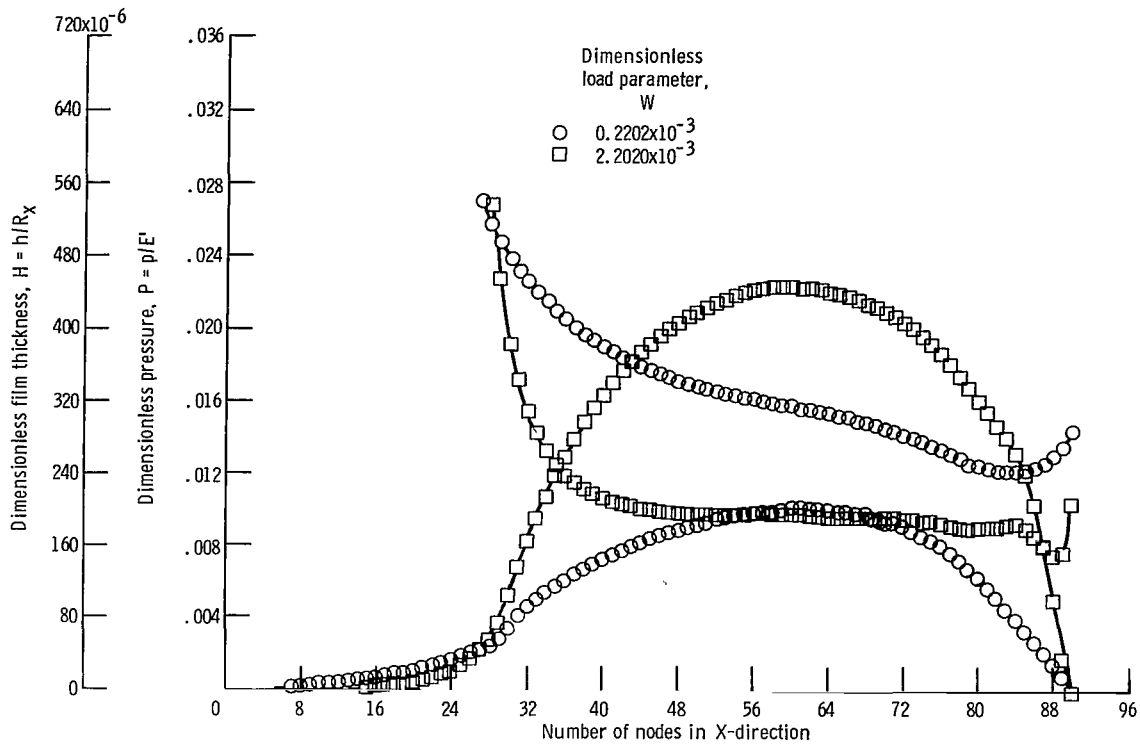


Figure 8. - Variation of dimensionless pressure and film thickness on X-axis for dimensionless load parameters W of 0.2202×10^{-3} and 2.202×10^{-3} . The value of Y is held fixed near axial center of contact.

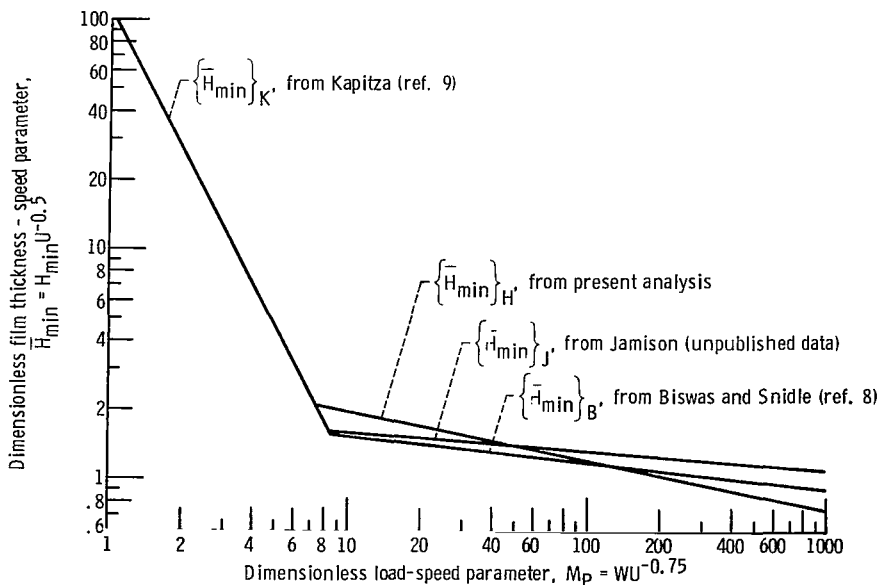


Figure 9. - Comparison of different investigators' results.

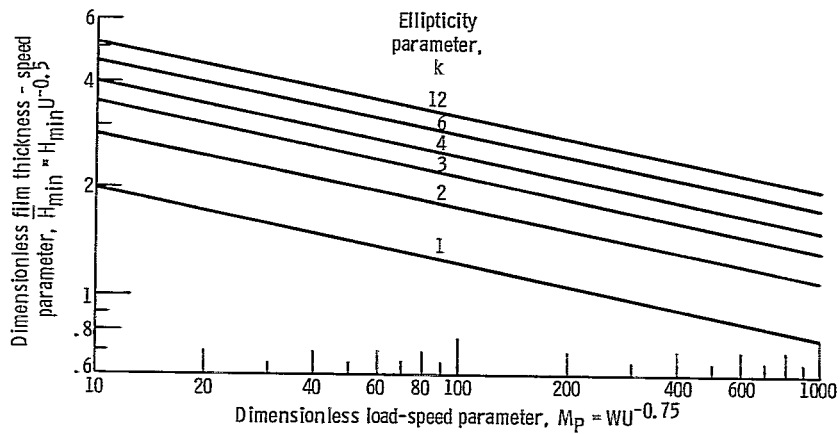


Figure 10. - Effect of dimensionless load-speed parameter on dimensionless minimum film thickness - speed parameter for six ellipticity parameter values.

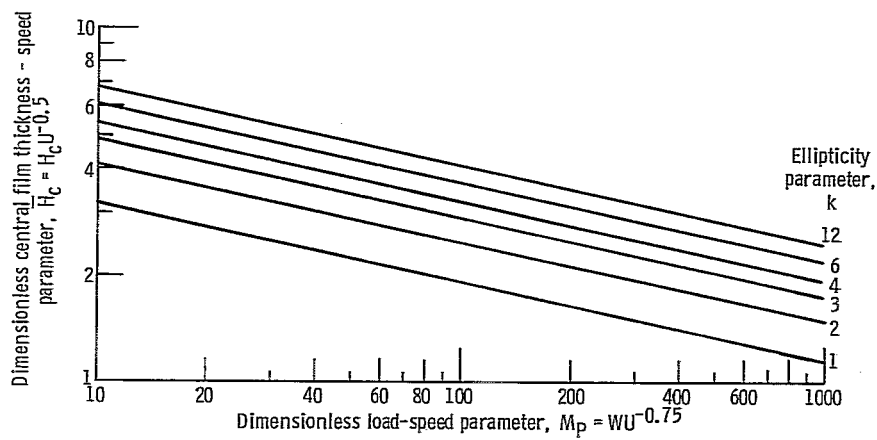


Figure 11. - Effect of dimensionless load-speed parameter on dimensionless central film thickness - speed parameter for six ellipticity parameter values.

NATIONAL AERONAUTICS AND SPACE ADMINISTRATION
WASHINGTON, D.C. 20546

OFFICIAL BUSINESS
PENALTY FOR PRIVATE USE \$300

SPECIAL FOURTH-CLASS RATE
BOOK

POSTAGE AND FEES PAID
NATIONAL AERONAUTICS AND
SPACE ADMINISTRATION
451



510 001 C1 U D 770715 S00903DS
DEPT OF THE AIR FCRCE
AF WEAPONS LABORATORY
ATTN: TECHNICAL LIBRARY (SUL)
KIRTLAND AFB NM 87117

POSTMASTER: If Undeliverable (Section 158
Postal Manual) Do Not Return

"The aeronautical and space activities of the United States shall be conducted so as to contribute . . . to the expansion of human knowledge of phenomena in the atmosphere and space. The Administration shall provide for the widest practicable and appropriate dissemination of information concerning its activities and the results thereof."

—NATIONAL AERONAUTICS AND SPACE ACT OF 1958

NASA SCIENTIFIC AND TECHNICAL PUBLICATIONS

TECHNICAL REPORTS: Scientific and technical information considered important, complete, and a lasting contribution to existing knowledge.

TECHNICAL NOTES: Information less broad in scope but nevertheless of importance as a contribution to existing knowledge.

TECHNICAL MEMORANDUMS: Information receiving limited distribution because of preliminary data, security classification, or other reasons. Also includes conference proceedings with either limited or unlimited distribution.

CONTRACTOR REPORTS: Scientific and technical information generated under a NASA contract or grant and considered an important contribution to existing knowledge.

TECHNICAL TRANSLATIONS: Information published in a foreign language considered to merit NASA distribution in English.

SPECIAL PUBLICATIONS: Information derived from or of value to NASA activities. Publications include final reports of major projects, monographs, data compilations, handbooks, sourcebooks, and special bibliographies.

TECHNOLOGY UTILIZATION PUBLICATIONS: Information on technology used by NASA that may be of particular interest in commercial and other non-aerospace applications. Publications include Tech Briefs, Technology Utilization Reports and Technology Surveys.

Details on the availability of these publications may be obtained from:

SCIENTIFIC AND TECHNICAL INFORMATION OFFICE

NATIONAL AERONAUTICS AND SPACE ADMINISTRATION

Washington, D.C. 20546